Dynamic light scattering on agitated granular media

Jan Philipp Gabriel[1,*], *Christopher* Mayo[1], *Marlo* Kunzner[1], and *Matthias* Sperl[1,2,**]

[1]Institut für Materialphysik im Weltraum, Deutsches Zentrum für Luft- und Raumfahrt (DLR), 51170 Cologne, Germany
[2]Department for Theoretical Physics, University of Cologne, 50937 Cologne, Germany

Abstract. Light scattering is an established measuring technique for colloidal and molecular systems to measure the translational and rotational dynamics [1]. For granular media, the situation is more difficult because the scattering mechanisms are more system-specific, and the short wavelength is more sensitive to shorter length scales than the investigated grain sizes. We discuss the possibility of using diffusing wave spectroscopy to extract particle velocities and inter-particle distances to obtain diffusion coefficients, as well as the limitations of this technique. The paper compares the analysis of a dense model system of 130 μm polystyrene spheres excited by a voice coil [2] and a piezo agitation [3, 4] setup, and discusses the experimental differences. These experiments have been conducted both on Earth and on board the International Space Station.

1 Introduction

It is challenging to observe the dynamics of densifying grains at a particle level since it is a slow, history-dependent process in a turbid 3D system. It is not possible to use classical observation with a camera and particle tracking in dense 3D bulk systems. Scattering is a well-established method for observing the dynamics of such systems. Specifically, light scattering can be used to observe sub-micrometer-scale dynamics in dense systems. The light scattering technique diffusing wave spectroscopy (DWS) was previously used on granular matter on strong and moderately agitated systems, like grains flowing through a funnel [5], on grains when fluidized by a gas flow with gravity (1g) [6] and in drop tower experiments without gravity [7]. For observing the slow densification of grains to reach glassy and jammed states in a controlled manner one can consider vibrations created by voice coils (VC)[2, 8] or piezo crystals (PZ)[3, 4] that can supply lower agitation to the system, like the funnel and gas fluidization. In this paper, we will compare these two vibrational agitation methods on a technical level. Therefore, we will focus on the modeling and analysis of the diffusing wave spectroscopy method to extract the mean square displacement (MSD) from the data. Finally, we will critically discuss the advantage of PZ agitation for preparing agitated dense systems of grains under low gravity conditions on board the ISS [4].

2 Experimental Approach

The test material for all experiments is a 5x15x15mm sample cell filled with 130 micrometer Polystyrene particles, which mimics both the volume and optical configuration
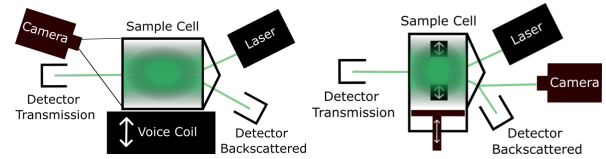
*e-mail: Jan.Gabriel@dlr.de
**e-mail: Matthias.Sperl@dlr.de

Figure 1. Vertical Voice Coil shaking agitation and emerged pulse Piezo agitation setup with detection by fiber optics and laser.

of the sample cells used on the ISS in the soft matter container [3]. Polystyrene will lose kinetic energy according to its coefficient of restitution of 0.64 [9]. The setups are schematically illustrated in 1, with a VC setup on the left and the PZ setup on the right side. The system includes a Verdi 5W λ = 532 nm Laser source (20-100mW used), fiber detection optics, and a camera in the VC setup for monitoring the density, and a camera like it is used on-board the ISS to detect multi-speckle DWS [2–4]).

We compare two agitation mechanisms with approximately 1g acceleration. The First approach is vertical VC shaking with amplitudes of 24 μm with a sinusoidal waveform at 100 Hz agitation frequency [2]. The Second approach is a periodic punch created by a rectangular profile with 2.2 μm amplitude by four piezo crystals. The crystals are evenly spaced in the sample volume with 1.5 mm space to the walls, each with a piezo volume of 2 mm^3 and 60 Hz contraction/expansion repetition rate [3, 4]. To extract the dynamics of the agitated system, we use light scattering. Since the system is strongly scattering in the Mie regime [10], we have to take advantage of the multiple scattering assumptions necessary for the DWS technique. The scattered light is collected by fiber optics and further split before being fed into Avalanche photodiodes (APDs), which avoids the phenomenon known as after-
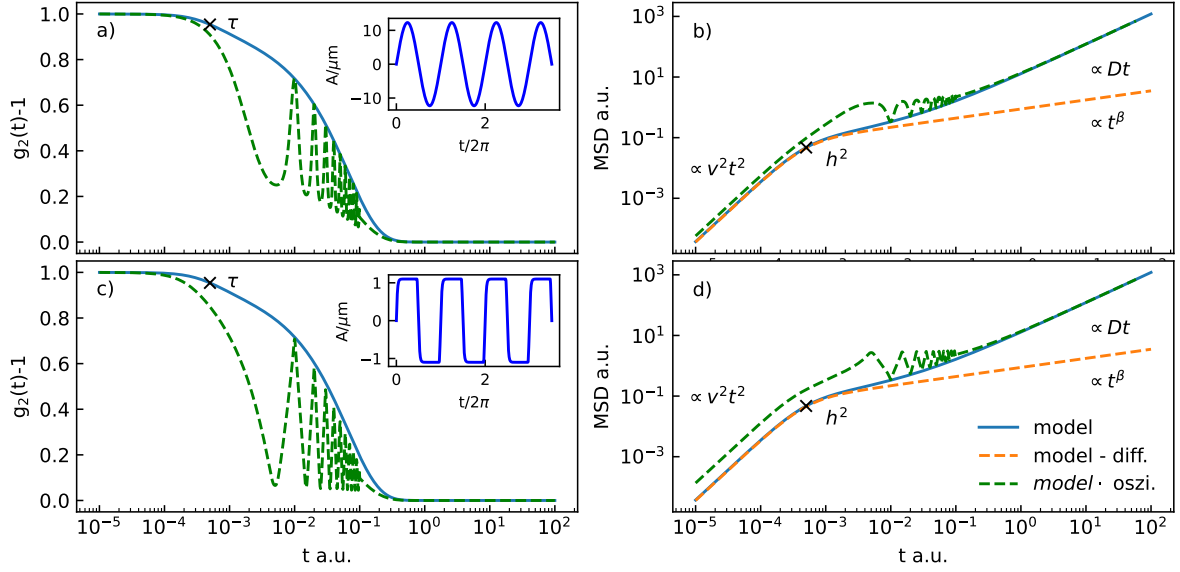
Figure 2. Schematic illustration of expected intensity correlation functions a) for sinusoidal oscillation and c) rectangular agitation with modeled MSD for b) voice coil and d) Piezo agitation. Green is the expected result, and blue is the reconstruction of underlying dynamics. Insets show a) the oscillation and c) rectangular agitation profiles with blue expansion.

pulsing. The measured time-resolved intensity fluctuations are hardware cross-correlated by an ALV USB 7004 correlator, resulting in g_2. For obtaining the electrical field correlation function $g_1(t)$ we can use the Siegert-Relation [1]

$$g_2(t) = 1 + \Lambda |g_1(t)|^2 \quad (1)$$

with Λ being a geometry factor close to one, in our case. The field correlation function g_1 can be connected to the mean square displacement $\langle r^2 \rangle$ with the DWS approximations [11, 12].

$$g_1(t) = \exp(-\frac{1}{3}\left(\frac{kL}{l^*}\right)^2 \langle r^2 \rangle) \quad (2)$$

with the wave vector $k = 2\pi/\lambda$, the optical path length L, the effective mean free path length $l^* = l/(1 - cos(\theta))$ where l is the mean free path length [2, 8]. For determining l we need the product of the volume fraction (VF) and the scattering cross-section $l(\sigma) = \frac{1}{\rho_N \sigma}$. This can be done in our case with Mie-Theory [10] and numeric calculation by a Python program PyMieScatt [13]. The MSD behavior can be modeled by power laws for ballistic, sub-diffusion, and diffusion parts according to [2, 4]

$$\langle \Delta x^2 \rangle = \frac{h^2}{(\frac{\tau}{t})^2 + (\frac{\tau}{t})^\beta} + 6Dt + 6D\tau \left(e^{-\frac{t}{\tau}} - 1\right) \quad (3)$$

with the end of the ballistic regime τ, the caging length h, and the power law exponent of the caging behavior β. The resulting MSD shape is illustrated in Fig. 2 with blue lines in b) and d). The measured intensity correlation function $g_{2,\mathbf{m}}$ is a weighted convolution between the oscillation $O(t)$ and the intensity correlation function $g_2(t)$, and the pure $g_2(t)$ correlation function.

$$g_{2,\mathbf{m}} = g_2(t)(CO(t) + (1 - C)) \quad (4)$$

In the case of the shaken cell, the convolution ratio is $C = 1$, and in the embedded case, most likely bigger than $1/2$, but in principle unclear. The oscillation in the decorrelation function $O(t)$ of the agitation is given by

$$O(t) = \frac{1}{T} \int_0^T \exp(-\kappa^2 A^2 [P(\omega(t + t')) - P(\omega t')]^2 dt' \quad (5)$$

with the agitation amplitude A, the period $T = 1/f$, the variance of final scattering vectors κ (depended on the detection geometry, approximately $0.002k$, details [2, 8]), the scattering geometry and the correlation of the periodic agitation function $P(t)$ as shown in the inset Fig. 2 a) sinusoidal and c) rectangular. The agitation depended prefactor $\kappa^2 A^2$ is handled as a fit parameter, due to the uncertainty of κ. The resulting modeled correlation functions with agitation and particle motion are the green dashed lines in Fig. 2 a) and c), and the MSD functions are in b) and d). The rectangular agitation method decays faster in the beginning than the sinusoidal waveform. The rectangular shape can produce a similar acceleration, but the amplitude can be a factor of 10 smaller. The diffusion case will not be reached in the presented data due to the focus on densifying systems, but can be observed with higher amplitudes as demonstrated in [2]. The correlation Function is calculated equidistant on a log scale, therefore, the correlation is undersampled at longer times when the point density is not high enough to resolve the periodic modulation. Additionally, after 200ms have elapsed, the correlation does not hardware-correlate single photon events anymore, but averages intensity values collected in a time interval. This is an unwanted but controlled averaging, changing the illustrated function in 2. This averaging decreases the resolvable MSD values.
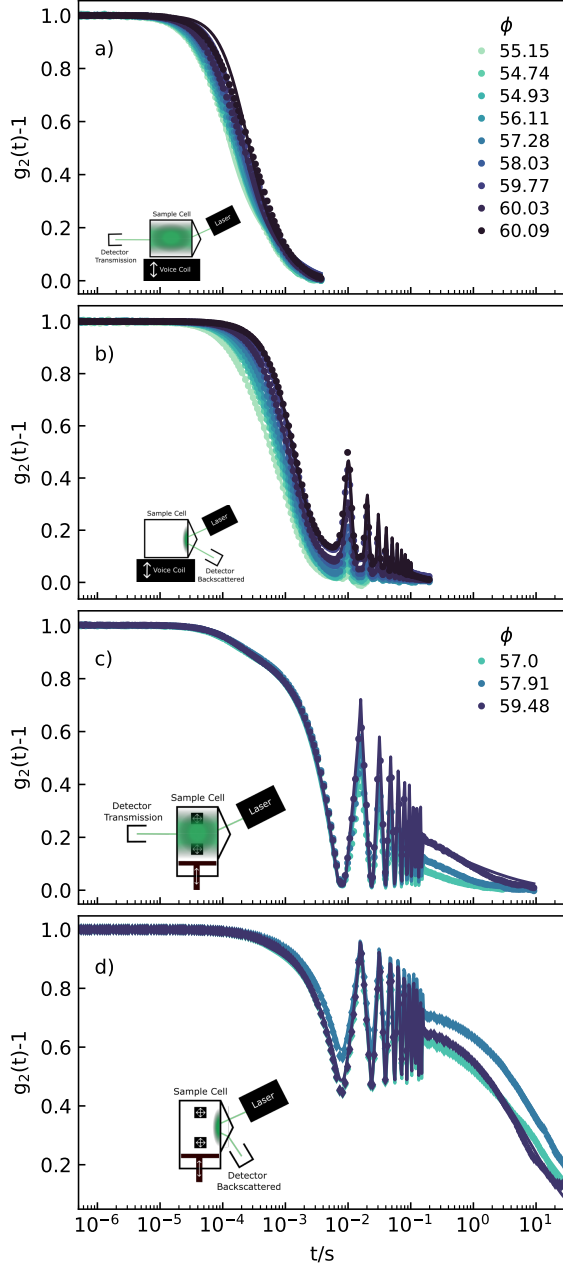
Figure 3. Density dependent intensity correlation function for Voice Coil agitation originating from a) bulk and b) wall as well as Piezo agitation originating from c) bulk and d) wall. Densification at approximately 0.9g. Straight lines described the model and dashed lines de-convoluted particle dynamics. Depictions illustrate agitation and measurement geometry.

Figure 4. Density dependent MSD function for Voice Coil agitating originating from a) bulk and b) wall as well as Piezo agitation originating from c) bulk and d) wall. Densification at approximately 0.9g. Straight lines described the model and dashed lines de-convoluted particle dynamics. Depictions illustrate agitation and measurement geometry.

3 Results

We shake and pulse our samples while determining g_2 for both the VC and PZ agitation as shown in Fig. 3 respectively. The measured correlation functions start close to one and decay to zero. For processing the correlation functions are normalized to one. The correlation functions in transmission geometry Fig. 3 a) and c) decay faster due to the longer light paths $L = 5$ mm resulting in more scattering events. The VC experiment shows a changing correlation function following the densification from volume
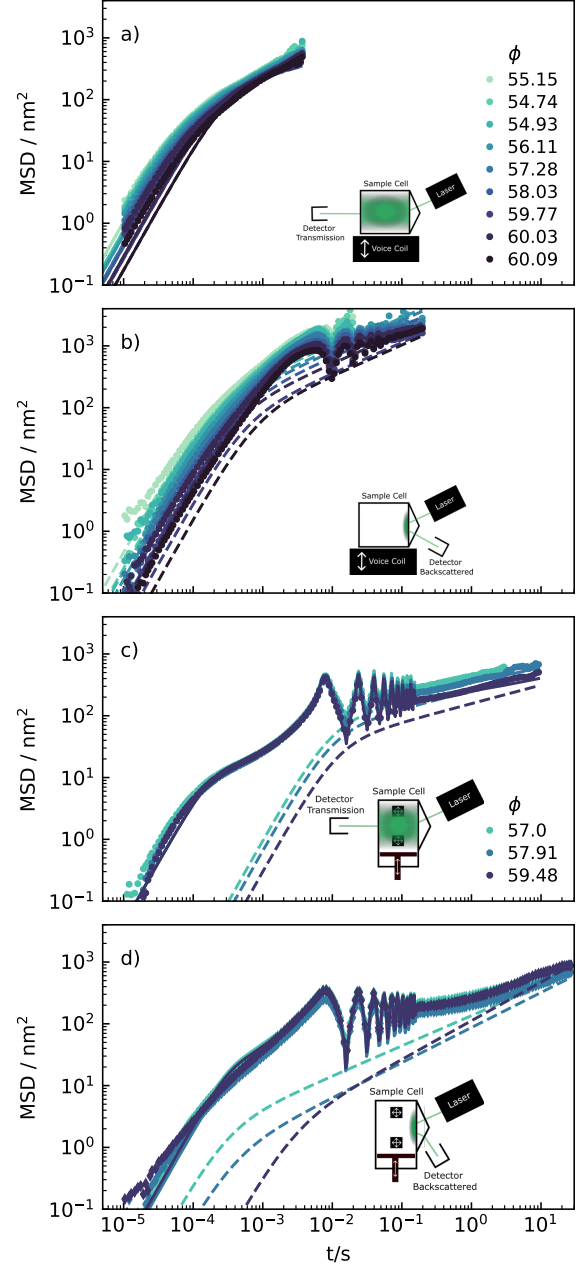
fractions of 55% to 60% determined from camera observation described in [2]. Since densification is less easy to determine precisely under gravity in the PZ cell, we only present g_2 for volume fractions of 57% to 59.5% in Fig. 3 c) and d) determined by setting the volume by the piston. The pulsed PZ agitation also slows down with densification. Despite similar acceleration, we observe a strong density dependency in the VC which we can not detect in the narrow volume fraction range of the PZ agitation. The PZ agitation distributes the forces more evenly in the sample resulting in vertical and horizontal agitation. The

backscattering dynamics appear slower due to the short optical path length $L = 2.5$ mm resulting in fewer scattering events decaying the correlation function. The dynamics originate from close to the wall and not from the bulk like in transmission geometry. All curves are well described by the fit functions when presented as correlation functions. This is not trivial because the fits are very sensitive to the correct shape and averaging implementation. Some influences are not strictly separable, the quality and long-time phase stability of the agitation signal, the determination of how much rest heterodyning the signal has, and the precise length L for backscattering geometry. In the DWS limit, the geometric Length L is only straightforward for transmission geometry.

4 Discussion

The intensity correlation functions g_2 and the fit functions are transformed into the MSD representation by eq. 2 and presented in Fig. 4. The critical value to determine the length scales of our MSD is σ which appears to result in a reasonable length scale, in regards to where the method should be sensitive. The products of $\kappa^2 A^2$ are in the order of one, as one would expect when the scattering cross-section σ is a good estimation. Both l and κ are sensitive to the same scattering cross-section. The scattering cross-section could be bigger due to the surface roughness of our particles, which would scatter more isotropically than the calculated Mie contribution for a perfect sphere.

The power law exponents β are fixed values of 1.3 and 0.5 for the separate graphs as indicated. These are common higher frequency behaviors in supercooled liquids before eventually ending in a diffusion-like behavior [14]. The VC amplitude is higher, which results in a faster decay compared to the PZ setup. When the oscillation is identifiable, the MSD delivers particle dynamics indicating that the caging dynamics of particles already start between 3 and 10 nm. For a clearer de-convolution of the fast particle dynamic and agitation is a small agitation amplitude desirable to imprint a weak agitation signal on the particle signal. The agitation is then quite weak if not boosted by pulsing, further complicating the analysis. The solution is then a combination of camera detection in which the oscillation can be removed in the process of calculating the correlation function [4].

We focused on analyzing and describing the fiber measurements. To follow the system when it becomes nonergodic, as to say approaching glassy behavior until it is jammed, these measurements need to be combined with camera measurements. This was done by conducting measurements on the ISS, where the described sample cell was used to observe glassy behavior until the system reached a final jammed state[4]. The glassy state was reached at an earlier VF in microgravity than in a 1g environment. Jamming has also been seen at a lower VF under microgravity conditions [4]. To probe longer length scales it is useful to explore the use of longer wavelengths in the THz regime [15].

References

[1] B.J. Berne, R. Pecora, Dynamic light scattering: with applications to chemistry, biology, and physics (Courier Corporation, 2000)

[2] M. Kunzner, C. Mayo, M. Sperl, J.P. Gabriel, The dynamics in vibro-fluidized beds: A diffusing wave spectroscopy study, arXiv: https://doi.org/10.48550/arXiv.2503.00517 (2025).

[3] P. Born, M. Braibanti, L. Cristofolini, S. Cohen-Addad, D. Durian, S. Egelhaaf, M. Escobedo-Sánchez, R. Höhler, T. Karapantsios, D. Langevin et al., Soft matter dynamics: A versatile microgravity platform to study dynamics in soft matter, Review of Scientific Instruments **92** (2021).

[4] C. Mayo, M. Kunzner, M. Sperl, J.P. Gabriel, Observing the glass and jamming transitions of dense granular material in microgravity, arXiv: https://doi.org/submit/6337664 (2025).

[5] N. Menon, D.J. Durian, Diffusing-wave spectroscopy of dynamics in a three-dimensional granular flow, Science **275**, 1920 (1997).

[6] N. Menon, D.J. Durian, Particle motions in a gas-fluidized bed of sand, Physical Review Letters **79**, 3407 (1997).

[7] P. Born, J. Schmitz, M. Sperl, Dense fluidized granular media in microgravity, npj Microgravity **3**, 27 (2017).

[8] T. Blochowicz, Jamming in granularen medien, Grundpraktikumsanleitung TU Darmstadt (2015), university of Darmstadt

[9] G. Constantinides, C.A. Tweedie, D.M. Holbrook, P. Barragan, J.F. Smith, K.J. Van Vliet, Quantifying deformation and energy dissipation of polymeric surfaces under localized impact, Materials Science and Engineering: A **489**, 403 (2008).

[10] G. Mie, Beiträge zur optik trüber medien, speziell kolloidaler metallösungen, Ann. Phys. **330**, 377 (1908).

[11] W. Brown, Dynamic Light scattering (Clarendon Press, 1993), chap. 16

[12] D. Weitz, J. Zhu, D. Durian, H. Gang, D. Pine, Diffusing-wave spectroscopy: The technique and some applications, Physica Scripta **1993**, 610 (1993).

[13] B.J. Sumlin, W.R. Heinson, R.K. Chakrabarty, Retrieving the aerosol complex refractive index using pymiescatt: A mie computational package with visualization capabilities, Journal of Quantitative Spectroscopy and Radiative Transfer **205**, 127 (2018).

[14] T. Böhmer, F. Pabst, J.P. Gabriel, R. Zeißler, T. Blochowicz, On the spectral shape of the structural relaxation in supercooled liquids, J. Chem. Phys. **162** (2025).

[15] P. Born, K. Holldack, Analysis of granular packing structure by scattering of thz radiation, Rev. Sci. Instrum. **88**, 051802 (2017).